DUJASE Vol. 6 (1) 30-37, 2021 (January)

Modeling and Simulation of Radial Temperature, Thermal Heat Flux, and Thermal Gradient Distribution in Solid and Annular Nuclear Fuel Element of Uranium Dioxide

Farhana Islam Farha and Md. Hossain Sahadath*

Department of Nuclear Engineering, University of Dhaka, Dhaka-1000

* *E-mail: hossain_ne@du.ac.bd*

Received on 14.01.21, Accepted for publication on 14.6.21

ABSTRACT

The solid and annular cylindrical nuclear fuel element comprising UO_2, Helium gas, and Zircaloy-4 typically used in Pressurized Water Reactors has been modeled using the engineering simulation software Ansys Mechanical APDL 17.0. Radial temperature distribution, as well as thermal heat flux distribution and thermal gradient distribution, have been simulated in the developed model by employing a linear solution. Results demonstrate that temperature distribution occurs in a bell-shaped manner radially across a solid fuel element, while maximum heat flux occurs at the inner surface of the cladding; and the pellet-cladding boundary regions are subjected to the highest amount of thermal gradient, and consequently, thermal stress. The heat flux and thermal gradient have been found higher for annular rod whereas solid fuel shows the higher fuel temperature. The developed model has been validated by analytically computing the temperature distribution of the same model, which showed a result analogous to the simulated result.

Keywords: Nuclear Fuel, Temperature, Heat Flux, Thermal Gradient, Ansys.

1. Introduction

In a nuclear power reactor, heat energy is generated in the nuclear fuel rods, which is then transferred to the coolant through the Helium gas gap and cladding regions by conduction, convection, and radiation. In this heat transfer, conduction plays a major part, while the contribution of the other two processes is minor. The main goal of the core thermal-hydraulic analysis is to ensure that the energy generated in the fuel is transferred to the coolant while keeping fuel rod temperature under limits in all possible steady-state and transient conditions, even in the scenarios of the worst possible accident [1]. Thus, the determination of temperature distribution in a fuel element, where maximum temperature among the whole reactor is reached, is of utmost importance. Thermal flux distribution is essential for the determination of the departure from nuclear boiling ratio or DNBR limit in pressurized water reactors which is the minimum ratio of the critical heat flux to the heat flux achieved in the core, while the assessment of thermal gradient indicates the thermal stress the fuel element is subjected to [2]. There have been a huge number of experimental and computational researches conducted to assess the thermal-hydraulic behavior of fuel elements in nuclear reactors using numerous software such as Fraptran, Frapcon, DUO_THERM, Ansys, etc. Before starting this particular study, previous works have been reviewed. In 1966, calculations of effects due to non-uniform distribution of heat generation, heat transfer coefficient, and fuel-cladding contact resistance were made in an analytical study on the temperature and heat flux distribution in nuclear fuel element rods [3]. Steady-state and transient analysis of heat conduction in nuclear fuel elements have been carried out in 2004 where a radial heat conduction model for fuel elements in fuel, cladding and the gap was developed [4]. Calculation of the temperature distribution in a TRIGA (**T**raining, **R**esearch, **I**sotopes, **G**eneral **A**tomics research reactor) type fuel element following the pulse operation was performed in 2004 [5]. In 2012, the heat flux and fuel temperature of an annular fuel rod were analyzed using a newly developed program, DUO_THERM [6]. A mechanism study and theoretical simulation on heat split phenomenon in dual-cooled annular fuel element were conducted in 2016 [7]. The effect of the central hole on fuel temperature distribution was investigated using the MARCODE software program in the MATLAB environment in 2017 [8]. Validation of results of analytical calculation of steady-state heat transfer in nuclear fuel element using ANSYS APDL was performed in 2018 [9]. Temperature drop along the radial axis was analyzed in steady-state heat transfer of nuclear fuel element using ANSYS APDL in 2018 [10]. In this paper, a model of a finite fuel element has been developed in the multiphysics software Ansys Mechanical APDL, in which steady-state thermal analysis is carried out to determine all three of the parameters, namely, temperature, thermal heat flux, and thermal gradient distribution in solid and annular nuclear fuel element of UO_2. A comparative study of solid and annular rod has also been given.

2. Materials and methods

Ansys is a 3D design and engineering simulation software. Ansys, Inc. is a public company that develops and markets multiphysics engineering simulation software for product design, testing, and operation. APDL is an acronym for Ansys Parametric Design Language, that allows the user to parametrize their model and automate common tasks. It is one of the most powerful commercial general purposes finite element programs on the market [11]. In this study, the finite element is performed in the steady-state environment of the Ansys Mechanical APDL 17.0. A thermal analysis calculates the temperature distribution and related thermal quantities in a system or component. Typical thermal quantities of interest are: the thermal temperature distributions, thermal gradients, thermal fluxes and the amount of heat lost or gained. To help establish initial conditions, engineers often perform a steady-state analysis before performing a transient thermal analysis. A steady-state analysis also can be the last step of transient thermal analysis, performed after all transient effects have diminished.

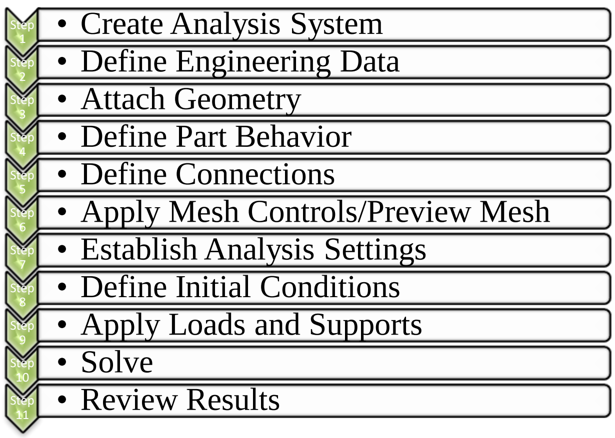

Fig. 1. Flow diagram for preparing the analysis model

Steady-state thermal analysis can be used to determine temperatures, thermal gradients, heat flow rates and heat fluxes in an object that are caused by thermal loads that do not vary over time. Such loads include convection, radiation, heat flow, heat fluxes and constant temperature boundaries. A steady-state thermal analysis may be either linear, which is the case in this study, with constant material properties; or nonlinear, with material properties that depend on temperature [12]. A flow diagram for preparing the Ansys model is shown in Fig. 1. Table 1 presents the basic pre-processing data (configurations of the geometry to be simulated) utilized for the generations of models in the present study.

Table 1. Specification of the models

Reactor Type	Pressurized Water Reactor (PWR)
Fuel material	Uranium Dioxide (UO_2)
Cladding material	Zircaloy-4
Fuel rod (solid) outer radius, R_{fo}	0.5334 cm
Fuel rod (Annular) outer radius, R_{fo}	0.5334 cm
Fuel rod (Annular) inner radius, R_{fi}	0.1601 cm
Outer to inner radius ratio, ($\alpha=R_{fo}/R_{fi}$)	3.33
Inner Cladding Radius, R_{ci}	0.5410 cm
Outer Cladding Radius, R_{co}	0.6019 cm
Thickness of Cladding	0.0609 cm
Coolant	Water

In the Ansys Mechanical APDL, the processing activites of the simuation includes, employing steady-state preference, development of a finite length of a cylindrical fuel element, as shown in Fig. 2. Initially, element type Solid- Brick 8 node 278 was selected as it is recommended for solid cylindrical object analysis, before providing input data of material properties such as thermal conductivity and density of the materials used. Then, in the modeling section, the geometry demonstrated in Fig. 2 was generated. The meshing of the volume created was performed using the mesh tool provided in Ansys Mechanical APDL 17.0. The meshing was done in a rather fine manner which results in three different meshed volumes (fuel, gas gap, and cladding materials), resulting in 99797 maximum number of nodes and 545760 maximum number of elements. The meshed volumes are demonstrated in Fig. 3. Afterward, thermal loads were put into the developed model. These loads were the volumetric heat generation rate in the fuel material and outer surface temperature of the cladding material. Finally, a linear solution was employed to solve and plot the temperature, heat flux, and heat gradient distribution across the fuel element. The application of the loads is shown in Fig. 4. The post-processing activities of the simulations are described in Section 3: Results and discussions part.

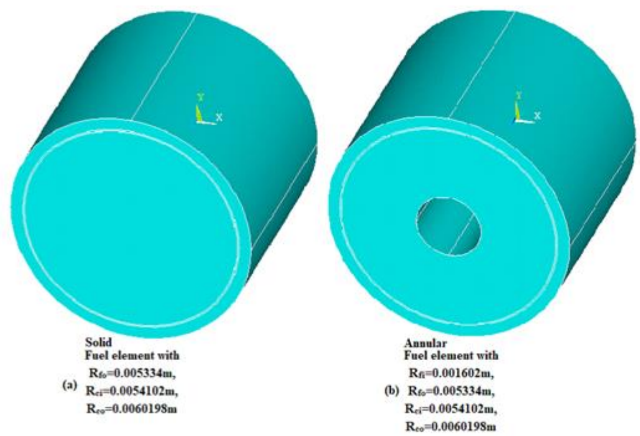

Fig. 2. Volume created for (a) solid and (b) annular fuel using Ansys APDL.

3. Results and Discussions

In the simulation using Ansys Mechanical APDL, radial temperature distribution, thermal flux distribution, and thermal gradient were analyzed. Contours as well as graphs of the aforementioned parameters were simulated. For fuel element with fuel and cladding with Helium gas gap in-between, contours in x, y, and z-directions were also illustrated. Average values of the thermal conductivity of the materials involved have been employed in these simulations.

3.1 Radial Temperature Distribution

Figures 5 (a) and (b) show the temperature contour and graph of fuel element with Helium gas gap obtained from simulation. The maximum fuel temperature is found to be 1960.87 K at the center of the fuel.

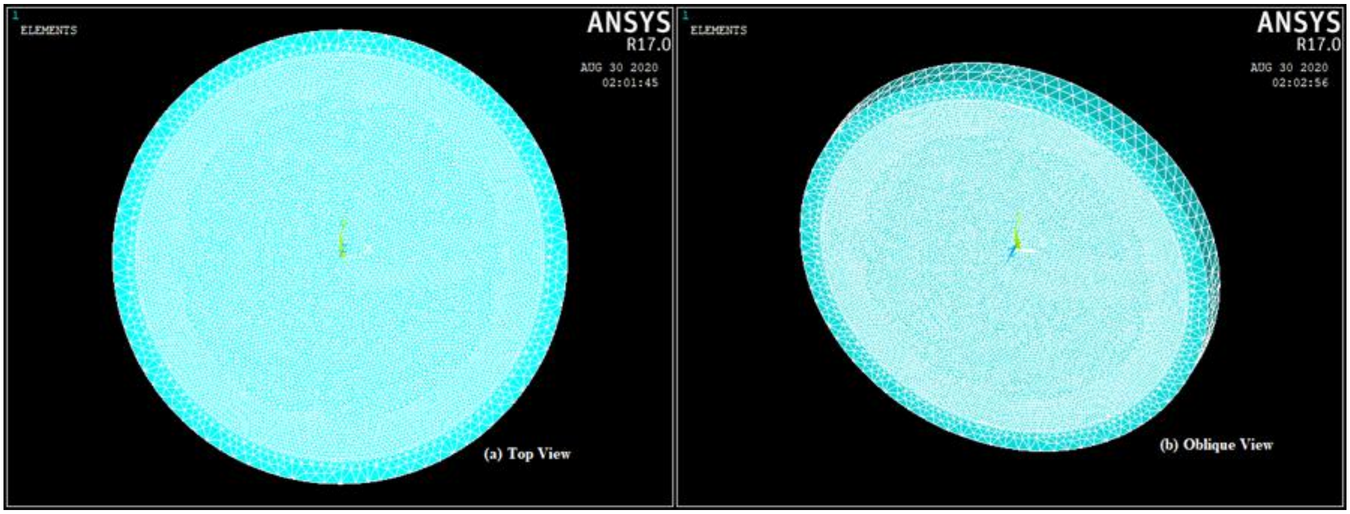

Fig. 3. (a) Top view and (b) oblique view of meshed volume

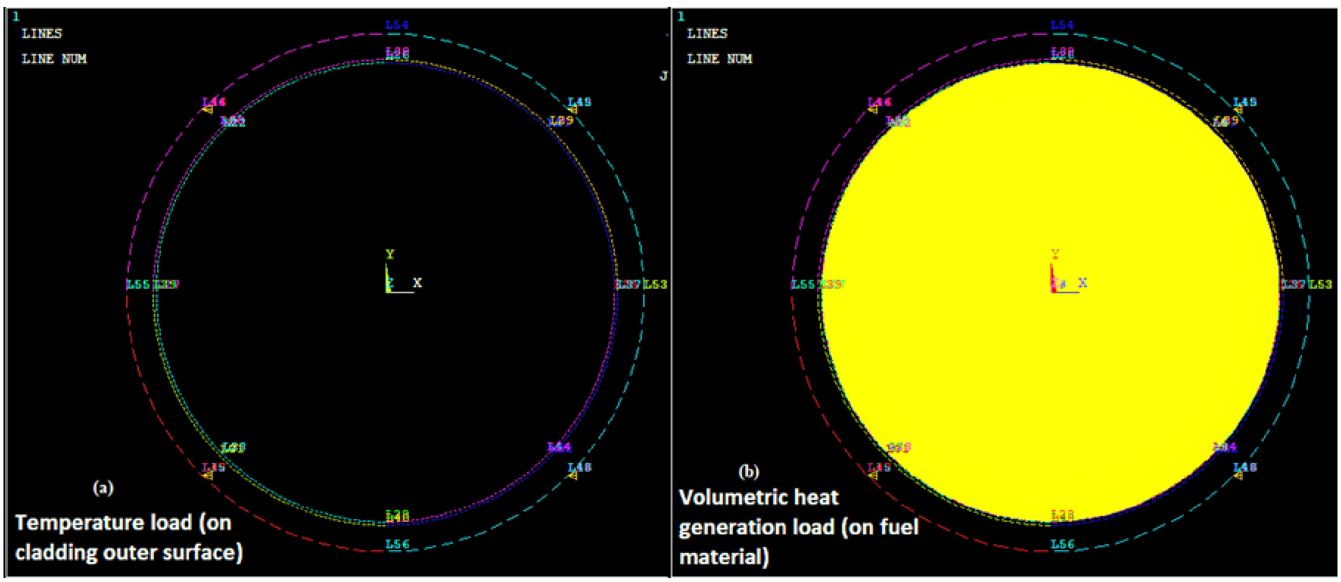

Fig. 4. Application of (a) temperature load and (b) volumetric heat generation load on the geometry

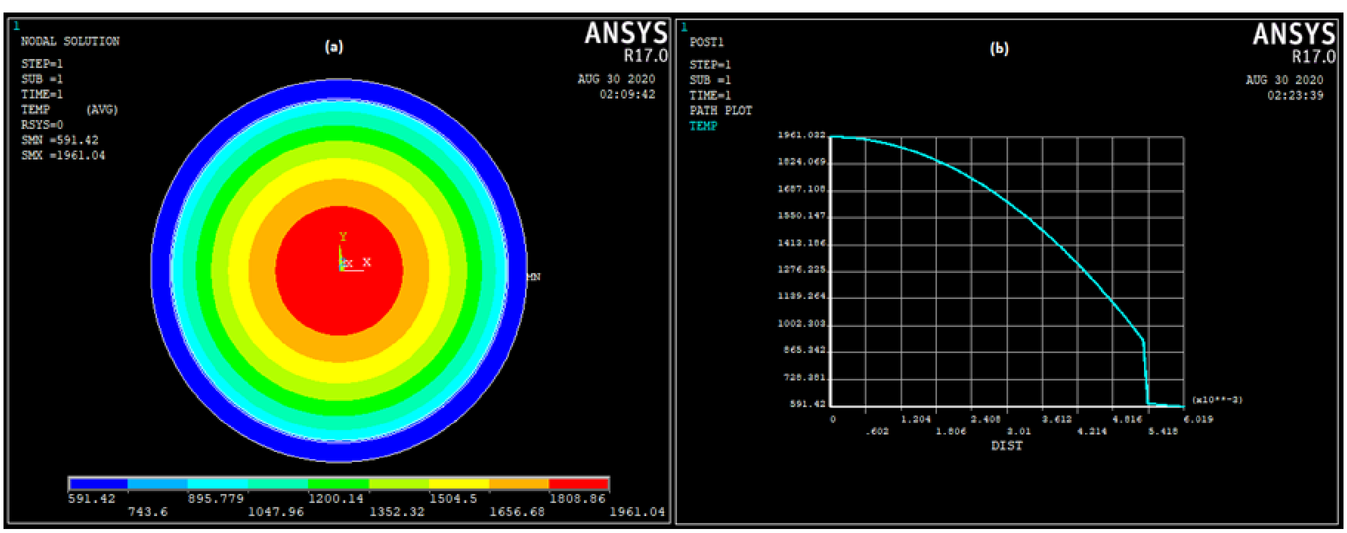

Fig. 5. Temperature distribution (a) contour and (b) graph of solid fuel element with UO_2 fuel, He gas gap, and Zircaloy cladding.

The temperature drop is highest in the Helium gas gap region. This can be explained by the low thermal conductivity of the helium gas which impedes the heat transfer. The shape of the graph is the same as that obtained from the analytical result shown in the section of result validation. The temperature contour consists of seven regions which represent a particular temperature range. The red zone corresponds to highest temperature zone followed by the lowered temperature zone.

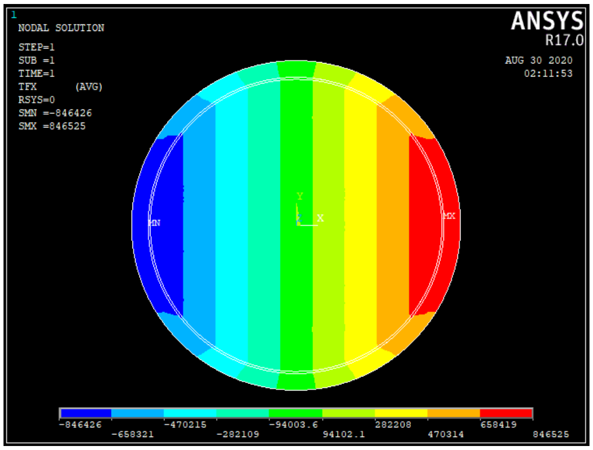

(a)

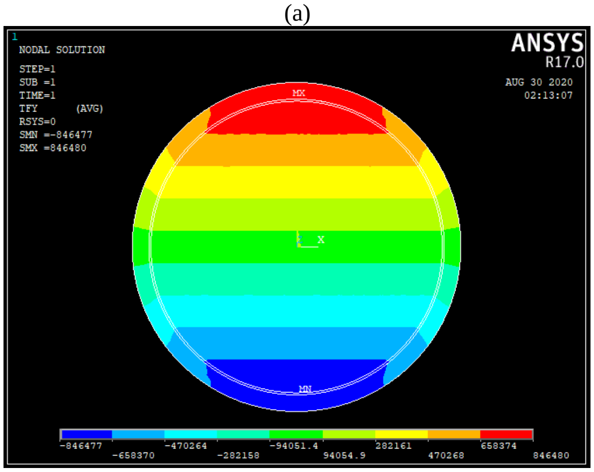

(b)

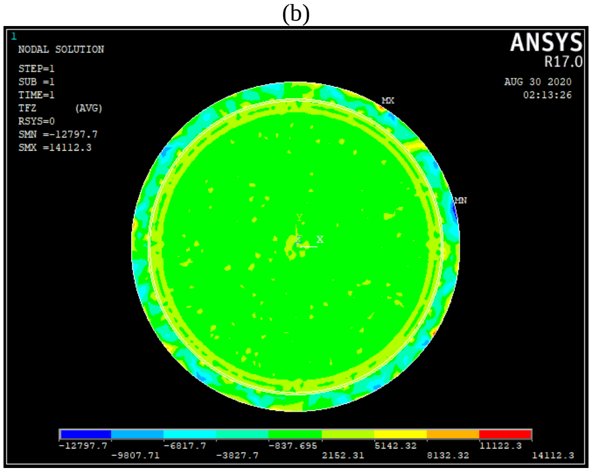

(c)

Fig. 6. Thermal flux contour in the (a) x-direction (b) y-direction and (c) z-direction of fuel element with UO_2 fuel, He gas gap, and Zircaloy cladding.

3.2 Thermal Flux Distribution

Variation of thermal flux in x-direction ranges from -846426 W/m^2 to 846525 W/m^2 according to Fig. 6 (a). As the distance increases radially in the x-direction, thermal flux also increases since the surface area is increasing due to the increasing radius of the fuel element. Thermal flux, as a result, is minimum in the center and maximum at the outermost surface, with an approximate symmetric distribution. Variation of thermal flux in y-direction ranges from -846477 W/m^2 to 846480 W/m^2 according to Fig. 6 (b). As the distance increases radially in the y-direction, thermal flux also increases since the surface area is increasing due to the increasing radius of the fuel element. Thermal flux, as a result, is minimum in the center and maximum at the outermost surface, with an approximate symmetric distribution. No symmetric variation of thermal flux can be observed in the z-direction as shown in Fig. 6 (c). The value of the flux ranges from -12797.7 W/m^2 to 14112.3 W/m^2 which is of a relatively smaller magnitude compared to that in the x and y-direction.

The vector sum contour of thermal flux in all directions is illustrated in Fig. 7(a). This contour represents a visual illustration of the variation of thermal flux in the fuel element. Thermal flux appears to be maximum at the outermost surface of fuel material with a value of 847270 W/m^2, while it has a minimum value of 3034.47 W/m^2 in the center. A graph of the overall vector sum of thermal flux is demonstrated in Fig. 7(b). It illustrates that gradually increases from a minimum value at the center to a maximum at the outer boundary of the Helium has gap region. After that, throughout the cladding region, there is a decrease in thermal flux.

3.3 Thermal Gradient Distribution

Fig. 8 (a) shows the variation of thermal gradient in x-direction ranges from -4220000 K/m to 4220000 K/m. However, across the fuel and cladding material, the magnitude of this gradient is negligible to that compared to the magnitude of thermal gradient the Helium gas gap region is subjected to. Analogous to the x-direction, variation of thermal gradient in y-direction also ranges from -4220000 K/m to 4220000 K/m according to Fig. 8 (b). Similarly, across the fuel and cladding material, the magnitude of this gradient is negligible to that compared to the magnitude of thermal gradient the Helium gas gap region is subjected to. The value of the thermal gradient in the z-direction ranges from -15393.8 K/m to 15638.4 K/m which is of a relatively smaller magnitude compared to that in the x and y-direction. Analogous to x and y direction, thermal gradient varies in a negligible range across fuel and cladding material, as well as in the gas gap region. This is shown in Fig. 8 (c). The vector sum contour of the thermal gradient in all directions is illustrated in Fig. 9(a). This contour represents a visual illustration of the variation of thermal gradient in the fuel element. The thermal gradient has a maximum value of 4230000 K/m in the center of the Helium gas gap, where temperature drop is the greatest. Throughout the other regions of the fuel element, the thermal gradient ranges from 1379.31 K/m to 470758 K/m.

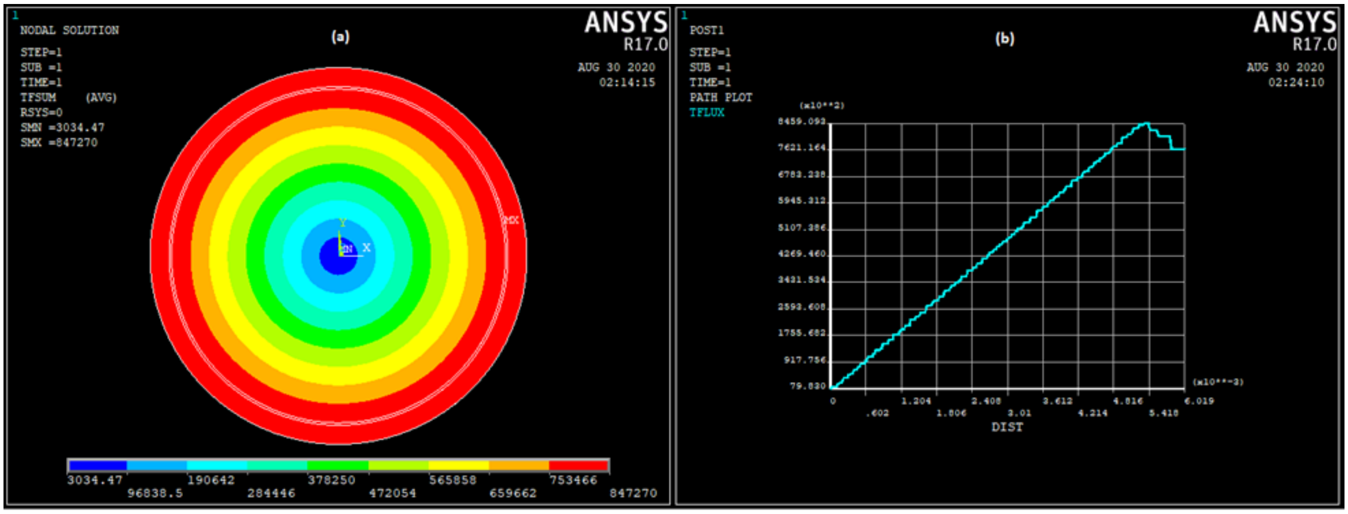

Fig. 7. Overall thermal flux (a) contour and (b) graph of fuel element with UO_2 fuel, He gas gap, and Zircaloy cladding.

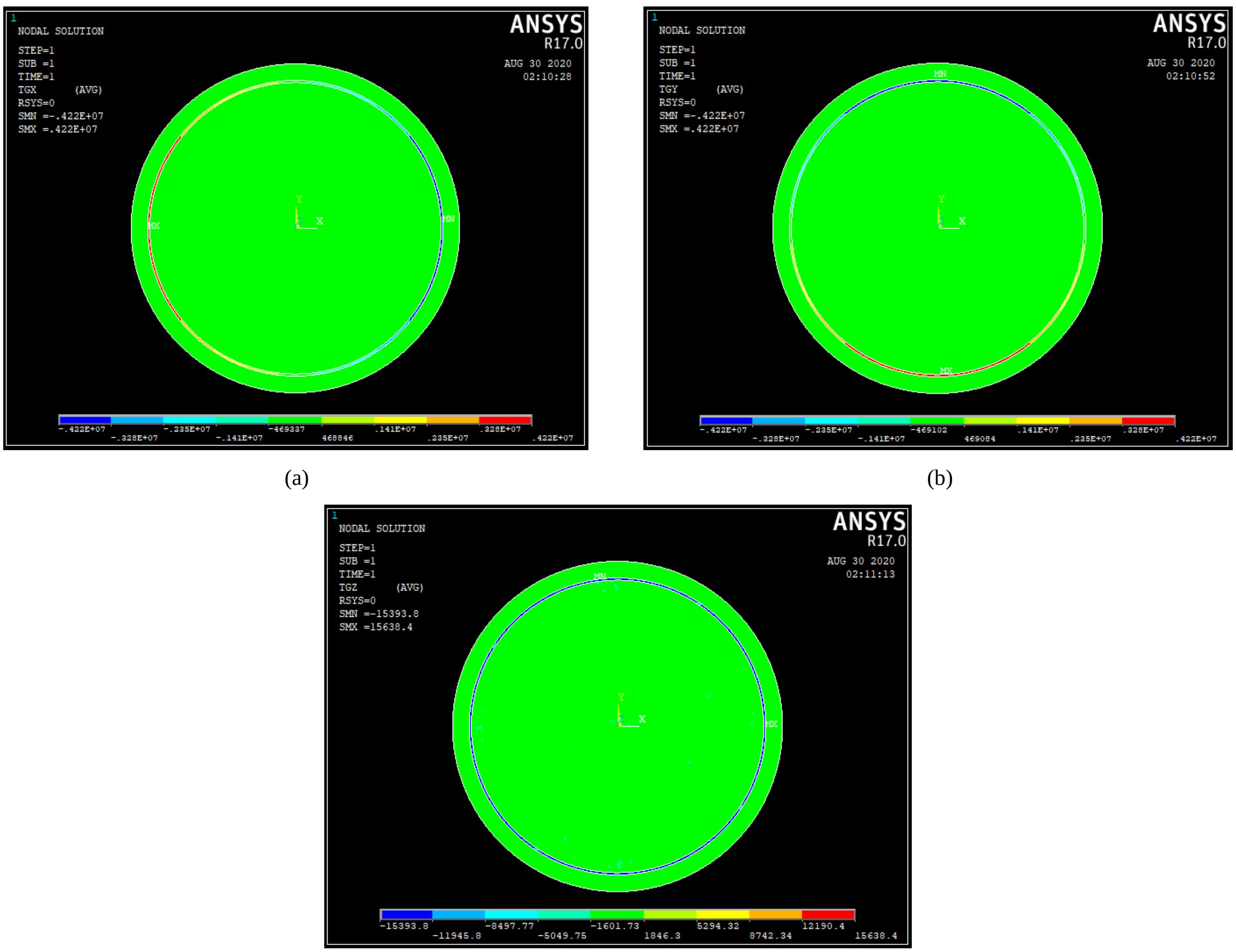

(a) (b)

(c)

Fig. 8. Thermal gradient contour in the (a) x-direction (b) y-direction and (c) z-direction of fuel element with UO_2 fuel, He gas gap, and Zircaloy cladding.

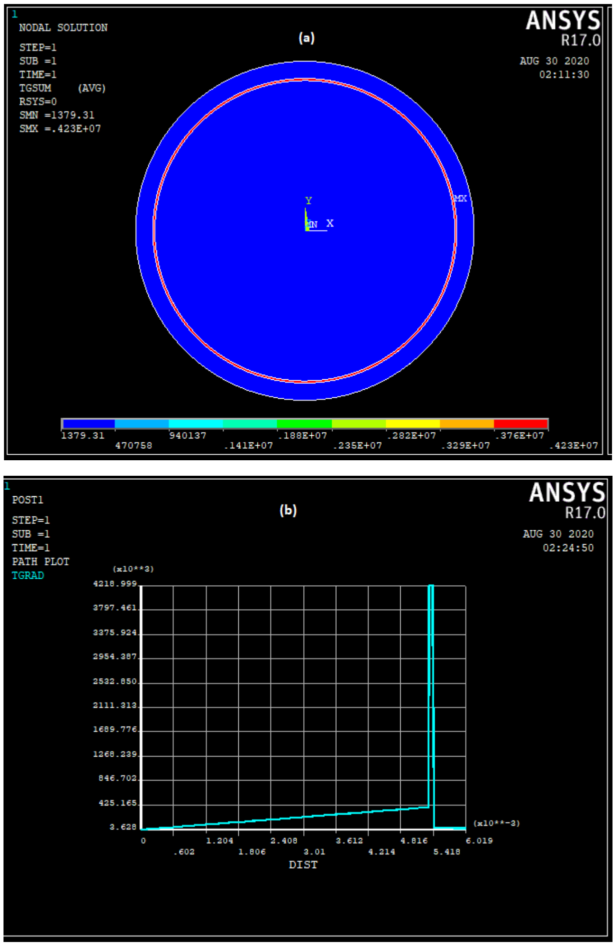

Fig. 9. Overall thermal gradient (a) contour and (b) graph of fuel element with UO_2 fuel, He gas gap and Zircaloy cladding

A graph of the overall vector sum of thermal gradient is demonstrated in Fig 9(b). It illustrates that with increasing radius, the thermal gradient is also increasing linearly up to the outer radius of the fuel material. After that, there is a surge in the thermal gradient in the Helium gas gap where it increases to a very high value and then decreases to a minimum value within a distance of 0.0000762 m (Helium gas gap thickness). Afterward, it remains constant throughout the cladding region. Thus, it can be said that the pellet-cladding boundary undergoes the highest amount of stress.

Fig. 10(a) and 10(b) show the temperature contour and graph of fuel element with an annular gap obtained from simulation using Ansys Mechanical APDL. The maximum fuel centerline temperature is found to be 1723.6 K. The temperature drop is highest in the Helium gas gap region. The vector sum of thermal flux in all directions is illustrated in Fig. 11(a). This contour represents a visual illustration of the variation of thermal flux in the fuel element. Thermal flux appears to be maximum at the outermost surface of fuel material with a value of 850130 W/m^2, while it has a minimum value of 38954.4 W/m^2 at the innermost surface of fuel material. A graph of the overall vector sum of thermal flux is demonstrated in Fig. 11 (b). It illustrates that with increasing radius, thermal flux is also increasing up to .003757 m. After that, there is a decrease in thermal flux until 0.004417 m. The vector sum of the thermal gradient in all directions is illustrated in Fig. 12 (a). This contour represents a visual illustration of the variation of thermal gradient in the fuel element. The thermal gradient has a maximum value of 4240000 K/m in the center of the Helium gas gap, where temperature drop is the greatest. Throughout the other regions of the fuel element, the thermal gradient ranges from 17706.5 K/m to 48685 K/m. A graph of the overall vector sum of thermal gradient is demonstrated in Fig. 12 (b). It illustrates that with increasing radius, the thermal gradient is also increasing linearly up to 0.005334 m. After that, there is a surge in the thermal gradient in the Helium gas gap where it increases to a very high value and then decreases to a minimum value within a distance of 0.0000762 m (Helium gas gap thickness). Afterward, it remains constant throughout the cladding region.

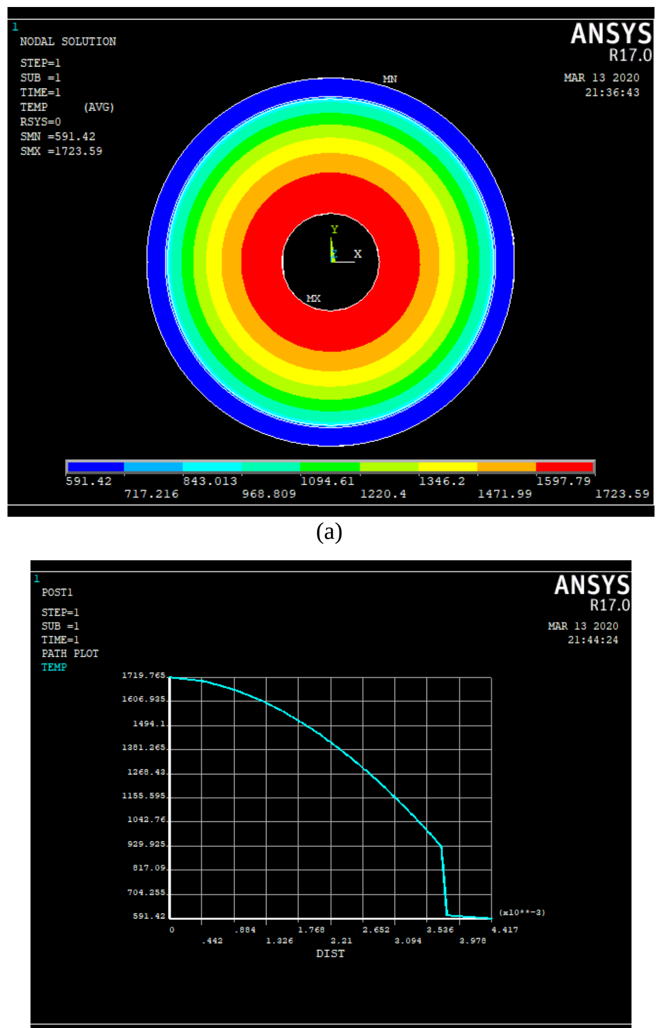

(a)

(b)

Fig. 10. (a) Temperature contour **(b)** Temperature distribution graph of fuel element with annular gap

An overall comparison of maximum thermal flux, minimum thermal flux, maximum thermal gradient, and minimum thermal gradient of the simulations conducted has been illustrated in Table 2. For the same PWR reactor, maximum thermal flux is highest when annular fuel pellets are used and lowest when pellets with no gaps are used. The minimum thermal flux is highest when annular fuel pellets are used and lowest when pellets with Helium gaps are used. Thermal gradients reach a very high maximum when there is a Helium gas gap used as opposed to when one is not used. This is due to the large temperature drop in the Helium gas gap. The minimum thermal gradient is lowest for pellets with fuel and cladding with Helium gap in between and highest for that with an annular hole.

Table 2. Simulated values for solid and annular rods

Fuel Element Type	Solid Rod	Annular Rod	Difference
Fuel Centerline Temperature (k)	1961.21	1714.93	246.28
Maximum Thermal Flux (W/m^2)	848356	850130	1774
Minimum Thermal Flux (W/m^2)	16459.6	38954.4	22494.8
Maximum Thermal Gradient (K/m)	4230000	4240000	10000
Minimum Thermal Gradient (K/m)	7481.6	17706.5	10224.9

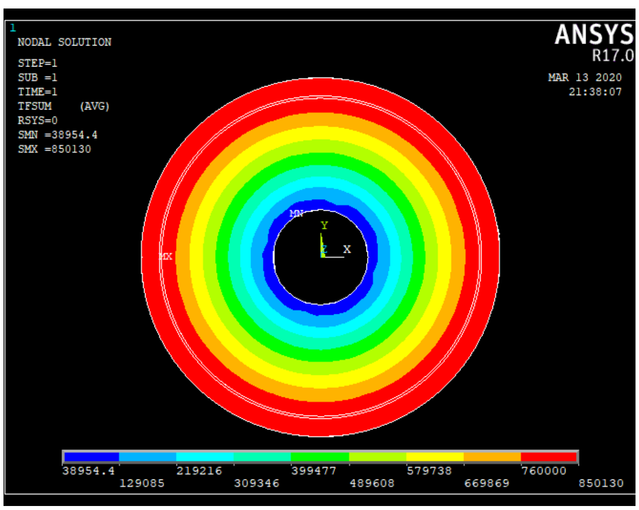

(a)

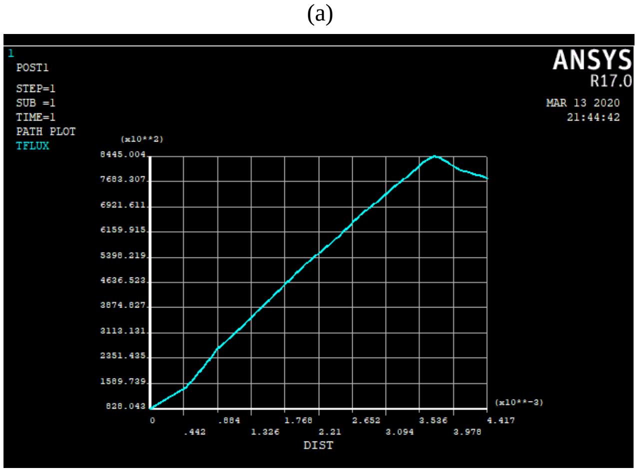

(b)

Fig. 11. (a) Thermal flux contour **(b)** Thermal flux graph of fuel element with an annular gap.

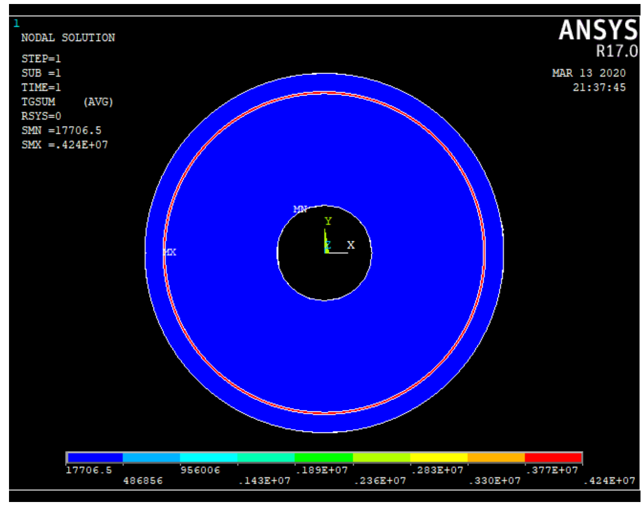

(a)

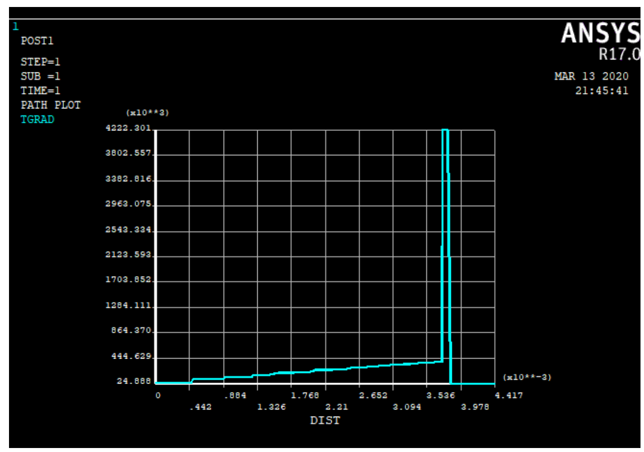

(b)

Fig. 12. (a) Thermal gradient contour **(b)** Thermal gradient graph of fuel element with an annular gap.

3.4 Analytical Validation of the work

The model developed in the Ansys Mechanical APDL 17.0 has been validated analytically using fundamental heat transfer laws and equations. Fourier's law and Newton's law of cooling are employed to compute temperature distribution across the cladding, Helium gas gap, and fuel element to fuel centerline [13, 14]. Figure 13 shows the analytical results for solid rods plotted using MATLAB. The curve is the same as that obtained from our model in Ansys. Agreement in the results of maximum centerline temperature obtained also ensures the validation of the whole study carried out so far.

A comparison of maximum centerline temperature found in analytical and simulation studies have been made in Table 3. The percentage difference between the values obtained by the two methods is very low ranging from 0.0173% to 0.505%. Thus it can be said that the analytical results obtained have been validated by the simulation results and vice versa.

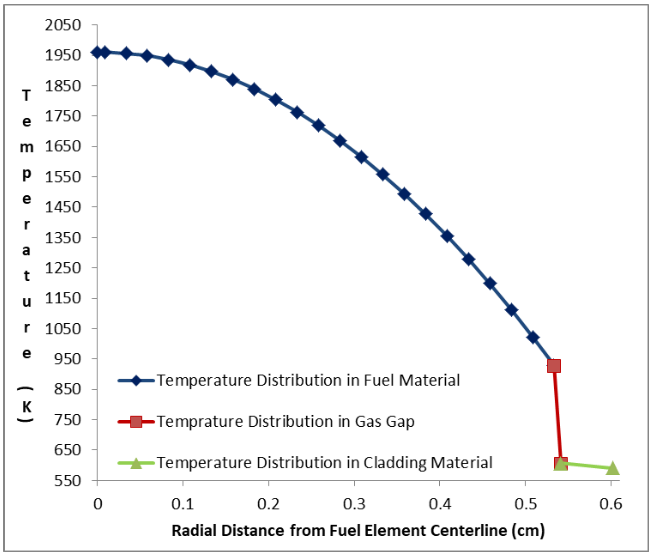

Fig. 13. Temperature (K) distribution graph of fuel element computed analytically.

Table 3. Comparison of analytical and simulation results

Fuel Element Type	Maximum Fuel Centerline Temperature (K)		
	Analytical	Ansys APDL	% difference
Solid Rod	1961.21	1960.87	0.0173%
Annular Rod	1714.93	1723.59	0.505%

4. Conclusion

In a cylindrical solid fuel element, temperature distribution occurs radially in a bell-shaped manner, with the highest temperature occurring at the center of the fuel material. Thus, the emphasis has to be given to designing and monitoring nuclear fuel temperature at the center of the fuel pellet. Thermal heat flux is maximum at the inner surface of the cladding, while lowest at the center of the pellet. The thermal heat flux value obtained from this model at the outer surface of the cladding is a factor of utmost importance as it is necessary for putting a limit to the DNBR for pressurized water reactors. Thermal gradient, as found in this study, tends to be highest at the gas gap region between the fuel and the cladding material. Thus, fuel outer surface and cladding inner surface is subjected to the highest level of stress. In comparison with solid rod, annular rod shows higher thermal flux alongside thermal gradient and lower fuel temperature.

References

1. Westinghouse Reactor Divisions, Westinghouse Electric Corporation. PWR Manual Nuclear Power Plant. Pittsburg, Pennsylvania, 1984.
2. J. J. Duderstadt, & L. J. Hamilton, "Nuclear reactor analysis", *New York: Wiley*, 1976.
3. R. Nijsing, "Temperature and heat flux distribution in nuclear fuel element rods: A Calculation of Effects Due to Non-uniform Distribution of Heat Generation, Heat Transfer Coefficient and Fuel-cladding Contact Resistance," Nuclear Engineering and Design, Volume 4, Issue 1, Pages 1-20, 1966.
4. R. Othman, Steady State and Transient Analysis of Heat Conduction in Nuclear Fuel Elements, Master's Degree Project, Department of Numerical Analysis and Computer Science, Royal Institute of Technology, Stockholm, Sweden, 2004. https://portal.tpu.ru/SHARED/k/KOROTKIKH/eng/Teaching/Tab/othman_rozhgar_04051.pdf
5. T. Biike Calculation of the Temperature Distribution in a TRIGA Type Fuel Element Following the Pulse Operation, Proceedings of the Third Eurasian Conference "Nuclear Science and its Application", Mugla University, Mugla, Turkey, October 5-8, 2004.
6. Y.-S. Yang, Y.-H. Koo, D.-H. Kim, J.-G. Bang, Y.-W. Rhee, D.-J. Kim, K.-S. Kim, K.-W. Song. "Thermomechanical Analysis and Irradiation Test of Sintered Dual-Cooled Annular Fuel," Nuclear Technology 178:3, pages 267-279, 2012.
7. Y. Deng, & Y. Wu, & Y. Li, Z., Dalin, T. XI, S. Guanghui, S.Z. Qiu, "Mechanism Study and Theoretical Simulation on Heat Split Phenomenon in Dual-cooled Annular Fuel Element," Annals of Nuclear Energy. 94. 44-54. 10.1016/j.anucene.2016.02.019, 2016.
8. M. Yarmohammadi, M. Rahgoshay, A. S. Shirani, "Effect of Central Hole on Fuel Temperature Distribution", *Nuclear Engineering and Technology*, Volume 49, Issue 8, Pages 1629-1635, 2017.
9. J. C. Odii1, E. B Agyekum, B. K. Afornu, M. N. S. Ansah, "Validation of Results of Analytical Calculation of Steady State Heat Transfer in Nuclear Fuel Element using ANSYS APDL", International Research Journal of Engineering and Technology (IRJET) Volume: 05 Issue: 01, January 2018.
10. J. Odii, A. Ephraim, A. Bright. Analysis of Temperature Drop Along the Radial Axis in Steady State Heat Transfer of Nuclear Fuel Element Using ANSYS APDL. 284-291, 2018.
11. M. K. Thompson, J. M. Thompson, "ANSYS Mechanical APDL for Finite Element Analysis", Elsevier Science, ISBN 9780128131107, 2017.
12. Ansys, Release 17.0, Help System, Mechanical APDL Documentation, ANSYS, Inc.
13. N.E. Todreas, M.S. Kazimi, Nuclear Systems: Volume 1. London: Taylor & Francis, 1990.
14. J.R. Lamarsh, A.J. Baratta, "Introduction to Nuclear Engineering. Third ed", *New Jersey: Prentice-Hall*, 2001.